Article

Computational Discovery of Inorganic Electrides from an Automated Screening

Computational discovery of inorganic electrides

Materials database → HT screening

Dimension distribution

0D 46.4%
2D 22.6%
1D 31.0%

Topological classification

TCI, TI, HSL_SM, HSP_SM, Trivial

Qiang Zhu, Timofey Frolov,
Kamal Choudhary

qiang.zhu@unlv.edu

HIGHLIGHTS

A descriptor was developed to identify the interstitial electrons in a material

The screening uncovers many potential inorganic electrides

There exists a strong correlation between electrides and topological materials

An automated computational scheme has been developed to screen the potential electride materials. This enabled a comprehensive search for the potential electride materials *in silico*. Many new candidate materials, with a variety of crystal packing and physical properties, were uncovered from a high-throughput screen of the existing inorganic materials database, which thus opens new avenues for future electride design.

2 **Benchmark**
First qualification/assessment of material properties and/or performance

Matter

CellPress

Article

Computational Discovery of Inorganic Electrides from an Automated Screening

Qiang Zhu,[1,4,*] Timofey Frolov,[2] and Kamal Choudhary[3]

SUMMARY

Electrides, with their excess electrons distributed in crystal cavities playing the role of anions, exhibit a variety of unique properties that make these materials desirable for many applications in catalysis, non-linear optics, and electron emission. While the first electride was discovered almost four decades ago, only few electride materials are known today, which limits our fundamental understanding as well as the practical use of these exotic materials. In this work, we propose an automated computational screening scheme to search for interstitial electrons and quantify their distributions inside the crystal cavities and energy space. Applying this scheme to all candidate materials in the Inorganic Crystal Structure Database, we report the identification of 167 potential electride materials. This work significantly increases the current library of electride materials, which enables an in-depth investigation of their chemistry-structure-property relations and opens new avenues for future electride design.

INTRODUCTION

Electrides represent a unique class of materials in which the excess electrons are trapped inside crystal cavities and serve as the anions.[1,2] Localization of electrons provides the early examples of quantum confinement. These trapped electrons in an electride are usually loosely bound and form unique interstitial energy bands around Fermi level, which dominates the transport and magnetic properties. Engineering on these energy bands can be used to design new materials with low work function and high carrier mobility, which make electrides attractive for various materials applications. While the first crystalline organic electride was made by Dye and coworkers in 1983,[3] the use of organic electrides for practical applications was limited by their thermal instability.[2] Significant progress toward the materialization of electrides was made by Hosono and coworkers.[4] Starting from the mineral mayenite ($12CaO \cdot 7Al_2O_3$), they synthesized the first room-temperature-stable inorganic electride $Ca_6Al_7O_{16}$ ($C12A7:2e^-$) via oxygen-reducing processes. Since then, $C12A7:2e^-$ has been used for ammonia synthesis[5–7] and as an electron-injection barrier material.[8] The discovery of $C12A7:2e^-$ has stimulated many new efforts to search for other inorganic electrides. Several new materials with improved functionality were developed in recent years.[9–19]

Our fundamental understanding of electrides has been greatly expanded in recent years thanks to the growing number of the discovered electride materials. Early discovered organic electrides exhibited very different magnetic properties ranging from almost no magnetism to having a strength comparable with $k_B T$ at room temperature, depending on the geometry of the trapped electrons.[2] Magnetic electrides were also reported in inorganic materials.[14,20,21] More recently, it has been suggested that electrides are suitable for achieving various topological phases in

Progress and Potential

Electride is a unique class of quantum materials in which excess electrons are trapped inside crystal cavities. Such exotic quantum confinement promises a variety of material applications. However, the research on electrides has been hindered by a relatively small number of available electride materials. Here, we present an approach that enables the automated identification of interstitial electrons in the potential electrides. Applying this approach to the known inorganic crystalline materials, we found hundreds of candidate electrides with substantial variability in chemical composition and crystal packing. Knowing their chemistry-structure-property relations will enable new avenues for future technological applications.

Matter

condensed matter physics, such as Y_2C,[22,23] Sc_2C,[23] Sr_2Bi,[23] Ca_3Pb,[24] Cs_3O/Ba_3N,[25] and Rb_3O.[26] Pressure has also proved to be an effective means to advance the electride research. For example, under compression, many simple metals (Li,[27,28] Na,[29] K[20]) and compounds ($NaHe_2$,[30] Mg_3O_2[31]) were found to adopt structures with valence electrons localized in the interstitial regions. These high-pressure electrides (HPEs) were shown to exhibit a variety of intriguing physical phenomena, such as metal-semiconductor-insulator transition[27–29,32] and superconductivity.[33]

In the past the identification of electrides required labor-intensive efforts, which included raw materials synthesis and sample characterization. Considering the current size of materials data (~30,000 after the removal of duplicates and structures with partial occupation) in the Inorganic Crystal Structure Database (ICSD),[34] it is impossible to investigate each compound by trial-and-error experiments. The high-throughput (HT) computational materials design, based on a search for target materials from a large database containing necessary thermodynamic and electronic properties for all available materials, has become popular in materials science in recent years.[35] To enable discovery of electrides with HT strategies one can proceed by (1) screening the materials with excess electrons localized in the crystal cavities and (2) identifying the real space and energy distribution of the interstitial electrons. In this work, we address this challenge by developing a set of reliable yet computationally feasible descriptors to quantify the interstitial electrons in a multidimensional space. Applying these descriptors to the existing ICSD materials included in the open database of Materials Project,[36] we report the identification of a subset of materials that possess interstitial electrons around Fermi level (E_F), 114 of which have not been considered in the previous literature. The total of 167 materials exhibits a diverse distribution in the chemical space and can serve as a guide for further in-depth studies.

RESULTS AND DISCUSSION

While in many cases materials can be simply classified by a single physical property (e.g., the band-gap values can be used to distinguish between metal, semiconductor, and insulator), a descriptor to distinguish electrides from other types of materials is not known at present. Several HT strategies for electride discovery proposed in the past included a search based on structural prototype,[16,17] identification of materials with strong electron localization in the interstitial space,[18] and the analysis of the partial density of states (PDOS) around E_F.[19] However, none of these approaches seem to provide a complete and accurate description of electrides. For instance, such strategies fail to identify the first experimentally established inorganic electride, C12A7. More extensive theoretical work on characterizing the electrides have been conducted recently.[37,38] Based on the previous work and our own analysis performed on the known electride materials, we summarize the three most important features of electrides: (1) interstitial electrons, (2) ionic bonding, and (3) floating around or adjacent to Fermi level. While the existence of interstitial electrons is certainly the most important descriptor for an electride, we emphasize that the presence of the other two features is equally necessary. The anionic nature makes the excess electrons intrinsically different from (nearly) free electrons in simple metals. Furthermore, these excess electrons need to float around Fermi level, so that they can contribute to low work function and high mobility, which are important for practical applications. Accordingly, we designed a computational screening strategy consisting of multiple steps including the analysis of electron localization function (ELF),[39] band structure, partial charge density, and PDOS, as shown in Figure 1. First, we analyze the ELF, as the existence of interstitial ELF maximum (regardless of its magnitude) can serve as the first evidence for an

[1]Department of Physics and Astronomy, University of Nevada, Las Vegas, NV 89154, USA

[2]Lawrence Livermore National Laboratory, Livermore, CA 94550, USA

[3]Materials Science and Engineering Division, National Institute of Standards and Technology, Gaithersburg, MD 20899, USA

[4]Lead Contact

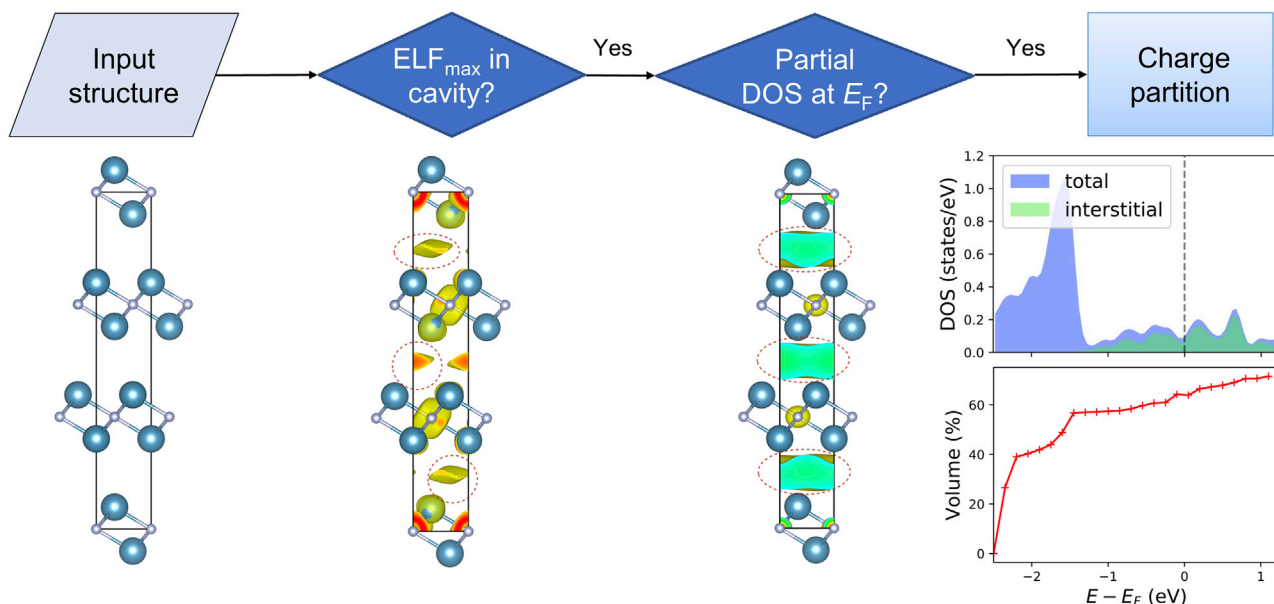*Correspondence: qiang.zhu@unlv.edu

https://doi.org/10.1016/j.matt.2019.06.017

Matter

CellPress

Figure 1. Computational Scheme for Inorganic Electride Identification

electride.[18,37] Second, we calculate the partial charge density of this compound at an energy range within $E_F \pm 0.05$ eV (see details in Supplemental Experimental Procedures). If there also exists charge maximum in the same interstitial region, we classify it as a possible electride and proceed to a more detailed analysis of the topology and energy distribution of the interstitial electrons. Following the Bader charge partition scheme,[40,41] we place the pseudo atoms to the sites of interstitial charge maxima, and partition the charge basin by assigning the boundary according the zero flux charge density gradient between the true and pseudo nucleus. Finally, we compute the density of states (DOS) and volume belonging to the interstitial sites and compare them with the totals. An ideal electride should occupy the entire volume of the crystal voids and make the primary contribution to the total DOS around E_F (as shown in Figure 1). In our calculations, we define the material as an electride when the interstitial electrons occupy at least a volume ratio of 5% at the energy range of $E_F \pm 0.05$ eV.

From the available materials data in the Materials Project database,[36] we made a query to obtain the first set of ICSD compounds by filtering out materials unlikely to be electrides (elemental solids or materials with band gap larger than 0.25 eV) or too expensive for calculation (e.g., materials containing more than 100 atoms in the primitive unit cell). This reduced the total number of candidate materials from 69,640 to 17,922. We then applied the computational scheme described above to search for the potential electrides from the reduced pool. The screening identified the total of 167 potential electrides distributed in a broad chemical space (see Figure 2), which included most of the previously discovered materials (a detailed comparison is included in Table S1). Among them, 112 were identified as electrides for the first time. Figure 2B shows that these materials constitute 59 elements out of the entire periodic table. It is interesting that many materials can be classified as intermetallics (e.g., Ca_3Ag_8, $Ca(MnAl_2)_4$, Dy_3Co, Yb_5Sb_3). This agrees with a recent HT survey[19] and experimental reports,[42,43] suggesting that intermetallics are a largely unexplored family of materials suitable for future consideration. Another important insight that can be gained from the elements distribution is that the excess electrons
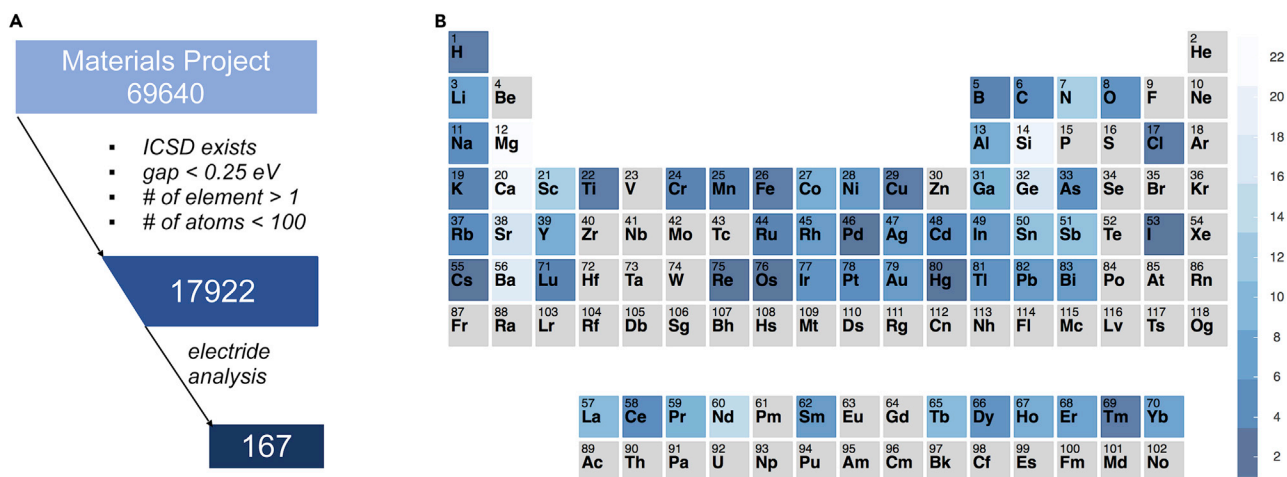
Matter

CellPress

Figure 2. Computational Screening of Electrides from the Inorganic Materials Database
(A) General screening strategy based on the available materials data.
(B) Distribution of chemical substances among the 167 electrides identified in this work.

are provided by elements with small electronegativity and large atomic radii, which typically appear in the alkali, alkaline earth, and early transition metals in group IIIB. Among them, the alkaline earth metals (Mg, 23; Ca, 21; Sr, 17; Ba, 19) occur more frequently than others.

Figure 3 shows further statistical analysis performed on the identified materials. In terms of stoichiometry, they include 103 binaries, 63 ternaries, and 1 quaternary. Since we are only interested in the materials that are recoverable at ambient conditions, the HPEs such as elemental Li, Na, and K are omitted in this library. We further classify the identified electrides according to the structural similarity. We found 48 distinct prototypes, 8 of which contain more than 5 materials (Mn_5Si_3: 38; HoMgSn: 14; Pr_2MgNi_2: 13; La_3In: 9; Pr_4MgRu: 7; Sr_2Bi: 7; Ca_2N: 7). Compared with the previous studies,[16–19,44] we have identified 25 new prototypes, suggesting that our descriptor is capable of discovering new classes of materials. Having identified 48 distinct prototypes, many more new electrides can be generated by chemical substitution approaches. For most materials the calculated formation energy was negative, with only few exceptions representing materials from high-pressure synthesis such as Rb_3Os, Ca_3Pb, Na_2Cl, and Na_3Cl_2. A better stability criterion is the normalized formation energy based on the distance to the convex hull (E_{hull}), which is the minimum energy of decomposition into an isochemical mixture of other phases.[45] In such convex hull construction, the stable compounds always have zero E_{hull} values, while the compounds with positive E_{hull} would decompose into the mixture of other neighboring compounds with zero E_{hull}. As shown in Figure 3D, the majority of compounds (116 out of 167) are thermodynamically stable against decomposition ($E_{hull} < 1$ meV/atom). However, E_{hull} itself only tells the thermodynamic preference of a compound in a closed system; the practical applications often require room-temperature stability in the presence of other environmental species (such as water and air). More extended stability analysis of these materials is a subject of future experimental investigation.

Figure 3E plots the distribution of the interstitial ELF maxima (ELF_{max}) for the identified electride materials. Interestingly, there is a wide spread in the calculated values ranging from as low as 0.26 up to the theoretical limit of 1.0. These data
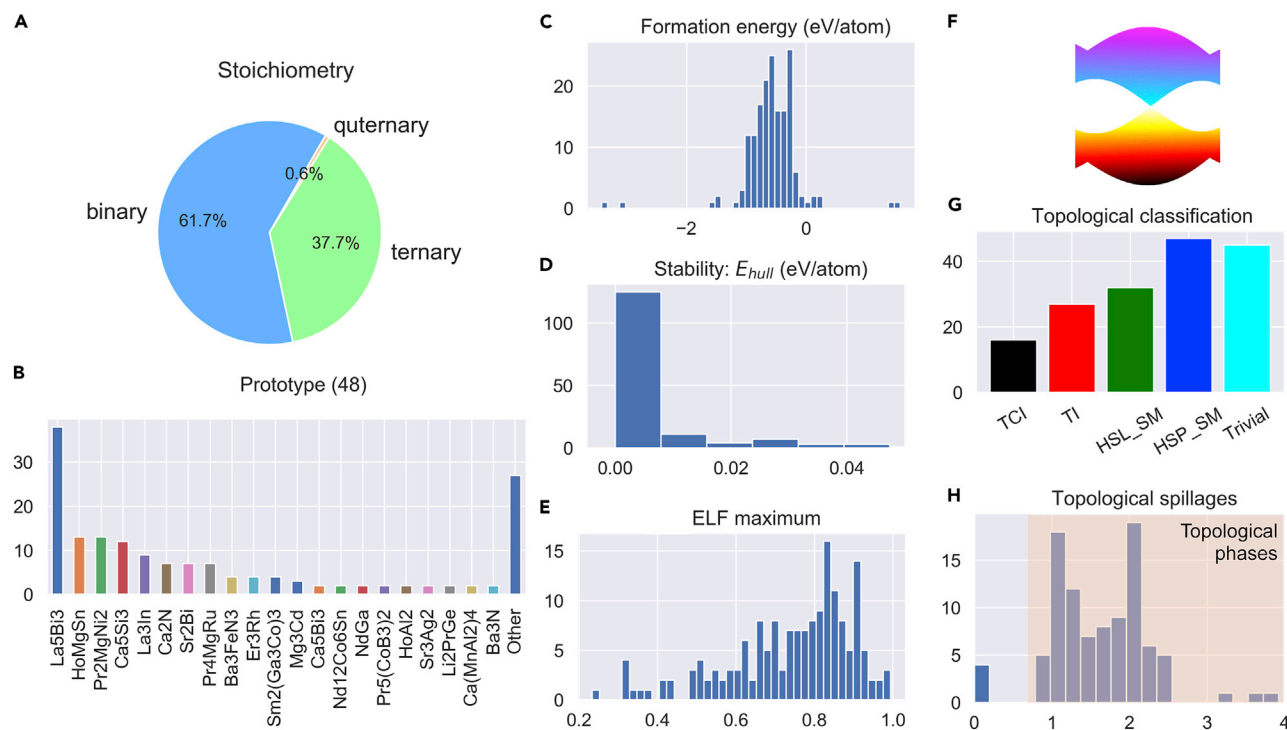
Figure 3. Statistical Analysis of the Selected Properties of the Identified 167 Electride Materials

(A) Distribution of stoichiometry.

(B) Distribution of structure prototype.

(C and D) Histograms of formation energy and stability based on the energy above the convex hull.

(E) Histograms of ELF maximum in the crystal cavities.

(F) Illustration of topological band inversion.

(G) Classification of topological materials, including topological insulator (TI), topological crystalline insulator (TCI), high-symmetry point semi-metal (HSP_SM), high-symmetry line semi-metal (HSL_SM), and trivial states.

(H) Histogram of calculated spillage values, in which a value larger than 0.5 indicates that the material is topological.

suggest that using an arbitrary value of ELF maximum[18] to screen for electrides can miss a lot of potential candidates. On the other hand, these strong non-nuclear ELF maxima do not always correspond to the DOS around the Fermi level (as will be shown in Figure 5). Although the strong ELF is not a necessary condition for an electride, the tendency of localization may be useful to predict the magnetic susceptibility. For electrides with electrons strongly localized in the dense interstitial sites, the orbital of interstitial electrons tends to behave like d-orbital, and thus favor magnetic ordering.[20,46] Indeed, some previously identified magnetic electrides have notably high ELF_{max}: Y_2C (0.87),[21] $Li_2Ca_3N_6$ (0.88),[47] and $K_4Al_3(SiO_4)_3$ (0.99).[48] Accordingly, we expect a large number of electrides identified in this work to possess antiferro- or ferromagnetism based on the analysis shown in Figure 3E.

Recent work suggested that the unique floating electrons in electrides are favorable for achieving band inversion for topological phases.[22,23] The automated classification of topological materials has been enabled recently based on the crystalline symmetries.[49–51] Comparing both the topological[49] and our electride materials databases, we found 122 materials belong to both catalogs (Figure 3F; for more details see Table S1), which include all the recently reported topological electrides Ba_3N, Cs_3O, Ca_3Pb, Y_2C, and Sr_2Bi.[22–25] Parallel with these efforts, we adopted an alternative approach of spin-orbit spillage, which has been established to identify many semi-metals, topological insulators, and topological crystalline insulators.[52]

Following the modified formalism used in JARVIS for density functional theory (JARVIS-DFT),[53] we calculated the spillage values for 96 materials based on the difference between non-spin-orbit coupling (SOC) and SOC wavefunctions for each material. A non-zero spillage value (generally larger than 0.5) indicates that the material is topological. Most of the electrides in Figure 3G have high spillage values. This clearly suggests that the identified materials are topological. Trivial materials such as Ca_2Sb (shown in Table S1) have spillage values close to zero. However, there are also a few cases where the symmetry indicator method[49] identifies the material as trivial but the spillage such as for Ho_4InIr. This might be due to difference in k-mesh used in the two methodologies. The apparent strong correlation between the electrides in chemistry and the electronic band topology in condensed matter physics may be useful for designing novel functional materials with combined properties in the future.

One of the key characteristics of electrides is the topology of the cavities confining the anionic electrons. In a zero-dimensional (0D) electride (such as $C12A7:2e^-$), the anionic electrons are localized in lattice cavities and isolated from each other, while in 1D, 2D, and even 3D electrides the electrons are connected along lattice channels or planes. Electrides with higher degree of connectivity are more desirable for catalytic and other applications. A variety of different geometries was found in the identified electrides, including 77 0D, 52 1D, and 38 2D electrides. Remarkably, we found several compelling materials reported for the first time. For example, the pore of sodalite type $K_4Al_3(SiO_4)_3$ has a diameter of 1.1 nm, which is about two to three times larger than that of C12A7. Interestingly, we also found that $Li_{12}Mg_3Si_4$ shares a similar crystallographic packing with C12A7. It is calculated to have about 2- to 3-fold higher excess charge densities than that of C12A7, which are thus promising to have higher mobility.[54] Our screening procedure has identified many other 1D and 2D electrides. For instance, $Nd_5(FeB_3)_2$ crystallizes in the same space group as Ca_2N (R-$3m$), representing another example of a 2D electride. Several representative materials are listed in Figure 4. The complete list can be found in Figures S2–S49 and Table S1.

It is important to note that crystal packing is not the only factor determining whether a given material is an electride; rather, it depends on a number of different factors. We illustrate the importance of chemical composition by a comprehensive investigation of the most common electride prototype Mn_5Si_3 (A_5B_3). According to the database, we found 105 such compounds in the ICSD. Our detailed calculation of partial charge density between ($-2.5 \leq E$-$E_F \leq 0$ eV) suggest that 94 of them have charge maxima inside the crystal cavities with the localized electrons forming 1D arrays along the (001) direction (Figure 5A). To investigate the energy distribution of these interstitial electrons, we calculated their PDOS based on Bader partition (see Supplemental Information). We found several types of PDOS profiles for these compounds, as shown in Figure 5B. For compounds such as Ba_5Sb_3, the PDOS peak of the interstitial electrons is very close to E_F, which is indicative of a *typical electride*. The second type of materials (such as Hf_5Si_3) has the PDOS peak at the deep energy bands away from the Fermi level. These materials are unlikely to be electrides since these excess electrons do not contribute to the DOS at E_F, and we therefore label them as *non-electrides*. The third type of materials (Pr_5Bi_3) has the PDOS peak close to E_F, leading to a small portion of PDOS to be present around E_F. We categorize them as *potential electrides* whose PDOS peak may be pushed to Fermi level due to external environments (e.g., pressure, temperature, chemical doping). We therefore place each compound in its PDOS peak position closest to E_F, with the size of each sphere representing the integrated PDOS value (i.e., the integrated Bader
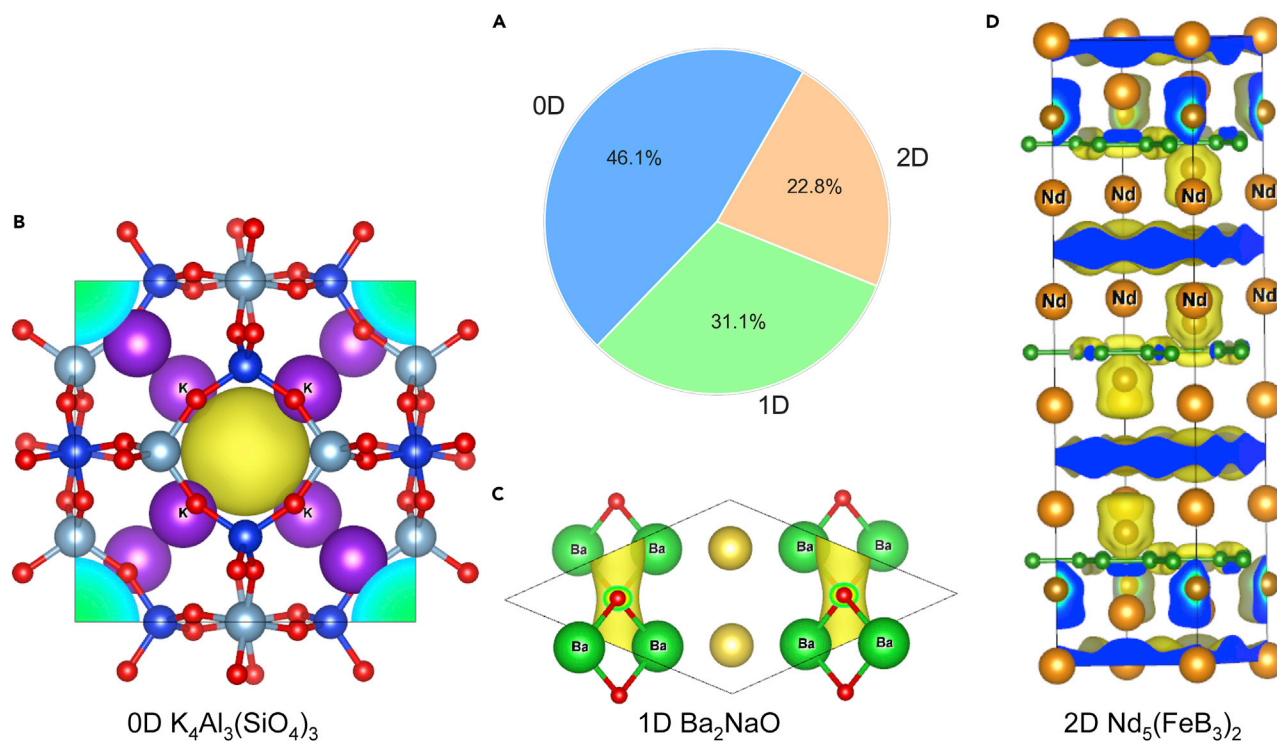
Figure 4. Example Electrides Categorized by the Dimensionality of the Interstitial Electrons
(A) Distribution of dimension among all identified electride materials.
(B) A representative 0D electride, $K_4Al_3(SiO_4)_3$.
(C) A representative 1D electride, Ba_2NaO.
(D) A representative 2D electride, $Nd_5(FeB_3)_2$.

charge) between -2.0 and 0 eV. As shown in Figure 5B, we can thus qualitatively draw a line to separate them by its electride properties. By analyzing their chemistry, we can clearly see that the non-electrides group is characterized by the compounds made of late transition metals such as Ta, Zr, and Hf. On the other hand, the group of typical electrides is composed of strong electron-positive elements such as Ba, Sr, Y, and many other lanthanides, while the materials close to the boundary also have elements with small electronegativity values occupying both A and B sites. Note that Y_5Si_3 from this family has been recently suggested to be a promising candidate material for practical application as it is water durable. However, its PDOS at E_F is relatively medium compared with other candidates. Such analysis, together with the 2D colored map (Figures 5B and 5C), can be instructive in guiding the development of new functional electrides in the future. Given that this type of material has not yet been thoroughly explored, many more electrides are yet to be discovered in the near future.

Compared with only a few dozen known electrides at ambient condition, we have identified 167 potential electride materials from a subset of ICSD materials. It is natural to ask why many electrides were neglected in the past. First, the traditional wisdom in electride design is to search for candidate materials from ionic solids with formal positive charges (e.g., Ca_2N[11]). However, we observed plenty of intermetallics in our database. This explains why a large quantity of electrides was missed in the past. Even for ionic solids, it is risky to gauge the formal charges purely from the chemical formula, as the atoms in the compound may adopt multiple valence states and adopt mixed chemical bonding.[54] For instance, it is difficult
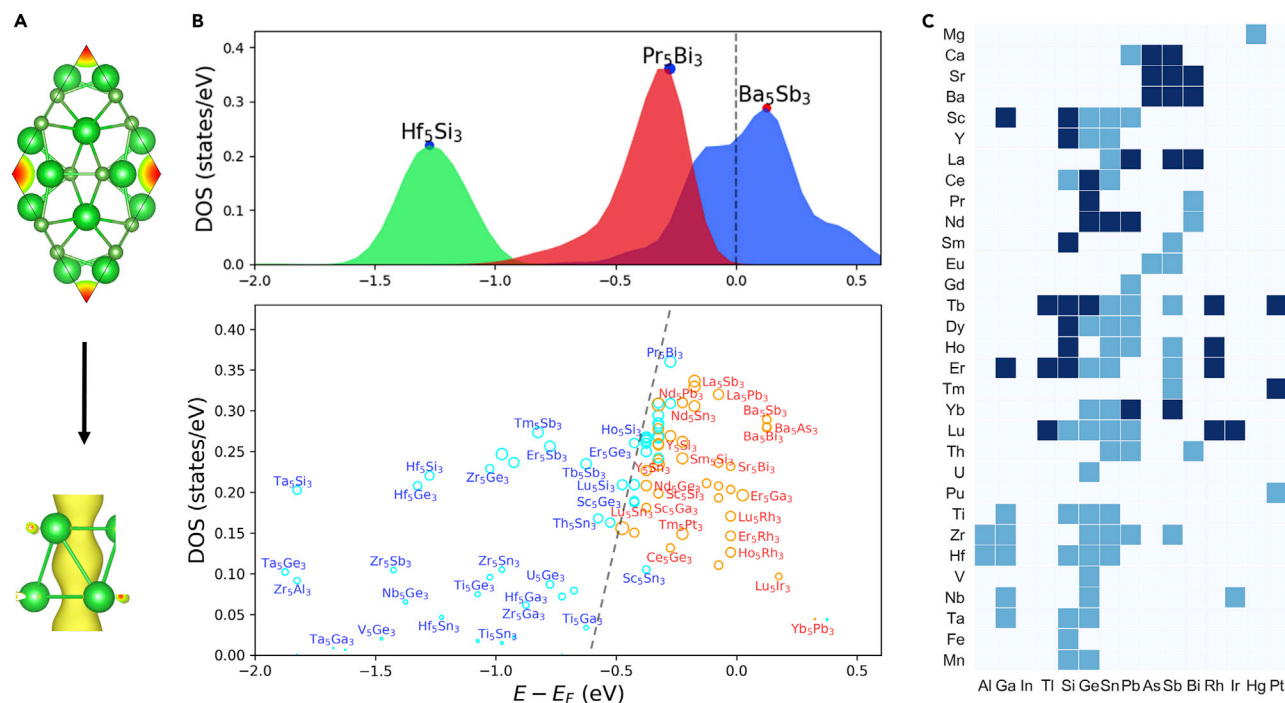
Figure 5. Statistical Analysis Performed for Mn$_5$Si$_3$-type Compounds

(A) Interstitial electrons in the crystal Ba$_5$As$_3$ (upper panel) and its local environments (lower panel).

(B) Energy distribution of the interstitial electrons in several representative materials for three different classes, namely non-electride, potential electride, and typical electride (upper panel), and the distribution of 105 Mn$_5$Si$_3$-type compounds reported in the ICSD separated by a schematic decision boundary (lower panel). In the lower panel, the cyan-colored points refer to the non-electride family while the orange points refer to the electride class according to our simulation. The size of each point represents the relative Bader charge. The materials close to the decision boundary will be considered to be potential electride class.

(C) Distribution of electrides in the 2D chemical space. Gray boxes indicate the absence of stable Mn$_5$Si$_3$ compounds for a given composition. Dark and light blue represents electrides and non-electrides, respectively.

to know whether Li$_2$Ca$_3$N$_6$ is an electron-rich compound without a detailed chemical bonding analysis.[55] Second, some materials (e.g., Ba$_2$NaO,[56] Li$_2$Ca$_3$N$_6$[47]) were characterized as electron-rich compounds in the literature although their electride properties were not examined in detail. Third, the past research primarily focused on developing the electride materials based on chemical substitution on the known prototypes (e.g., Mn$_5$Si$_3$, Ca$_2$N). Discovering new structural prototypes was limited because of the lack of efficient computational approaches. Lastly, it is important to acknowledge that most of the electrides are likely to be stable at only low temperature due to the presence of highly mobile electrons. Although most of the reported materials in this work are calculated to be thermodynamically stable (zero energy above the convex hull at zero temperature) in a closed system, they may quickly react with environmental species such as water and air. Therefore, it is possible that they were neglected due to the issue of instability. We believe the large quantities of electrides from our screening will provide an invaluable guide for future study of electrides toward materials discovery with enhanced stability and physical properties.

Conclusion

In sum, we propose a robust descriptor that can be used to identify the excess electrons in the electrides. With this methodology we search for electrides that contain interstitial electrons floating around the Fermi level by screening a large number of materials available through the ICSD. Our search yields 167 electrides including

Matter

previously experimentally identified electrides. Among them, 112 new materials and 25 new structural prototypes are reported for the first time. The identified electrides show substantial variability in their chemical composition and crystal packing, demonstrating the power of HT methods to discover novel electrides. Extending this search to more materials (e.g., inorganic wide-gap semiconductors,[57] insulators, and organic compounds[37]) would be the subject of future work. In addition, we believe that the descriptor proposed in this work can be also used to identify the electride materials from a more extended first-principles crystal structure search.[14,18] The drastically increased library of electride materials will benefit a broad range of potential applications of electrides, which include catalysis, non-linear optics,[58,59] and electrics.[60]

EXPERIMENTAL PROCEDURES

We performed the characterization of electrides based on density functional theory using the plane wave code VASP.[61] (Please note that commercial software is identified to specify procedures. Such identification does not imply recommendation by the National Institute of Standards and Technology.) The exchange-correlation functional was described by the generalized gradient approximation in the Perdew-Burke-Ernzerhof parameterization (GGA-PBE).[62] Using the parameter sets provided by Pymatgen,[63] we performed geometry relaxation (MPRelaxSet) and static (MPStaticSet) calculations for each selected structure, followed by the ELF and partial charge density calculation as described in Figure 1. To compute the PDOS, we used a reciprocal density of 250 for the first stage of screening and 500 for more accurate analysis at the second stage of characterization. The PDOS for the excess electrons are computed based on Bader grids as described in Section 1 of Supplemental Information. The structure prototypes were classified through the anonymous structure matcher utility in Pymatgen.[63] For the identification of topological materials, we searched for materials with large changes in the occupied wavefunctions due to including spin orbit coupling.[52,53] Alternatively, the online database for topological materials classification (http://materiae.iphy.ac.cn) was used for further comparison.

SUPPLEMENTAL INFORMATION

Supplemental Information can be found online at https://doi.org/10.1016/j.matt.2019.06.017.

ACKNOWLEDGMENTS

AUTHOR CONTRIBUTIONS

Q.Z. designed the research. Q.Z., T.F., and K.C. performed and analyzed the calculations and contributed to interpretation and discussion of the data. Q.Z. wrote the manuscript.

Matter

CellPress

DECLARATION OF INTERESTS

The authors declare no competing financial interests.

REFERENCES

1. Dye, J.L. (1990). Electrides: ionic salts with electrons as the anions. Science 247, 663–668.

2. Dye, J.L. (2009). Electrides: early examples of quantum confinement. Acc. Chem. Res. 42, 1564–1572.

3. Ellaboudy, A., Dye, J.L., and Smith, P.B. (1983). Cesium 18-crown-6 compounds. a crystalline ceside and a crystalline electride. J. Am. Chem. Soc. 105, 6490–6491.

4. Matsuishi, S., Toda, Y., Miyakawa, M., Hayashi, K., Kamiya, T., Hirano, M., Tanaka, I., and Hosono, H. (2003). High-density electron anions in a nanoporous single crystal: $[Ca_{24}Al_{28}O_{64}]_4+(4)e^-$. Science 301, 626–629.

5. Kitano, M., Inoue, Y., Yamazaki, Y., Hayashi, F., Kanbara, S., Matsuishi, S., Yokoyama, T., Kim, S.W., Hara, M., and Hosono, H. (2012). Ammonia synthesis using a stable electride as an electron donor and reversible hydrogen store. Nat. Chem. 4, 934–940.

6. Kuganathan, N., Hosono, H., Shluger, A.L., and Sushko, P.V. (2014). Enhanced N_2 dissociation on Ru-loaded inorganic electride. J. Am. Chem. Soc. 136, 2216–2219.

7. Hayashi, F., Tomota, Y., Kitano, M., Toda, Y., Yokoyama, T., and Hosono, H. (2014). Nh2-dianion entrapped in a nanoporous 12CaO 7Al2O3 crystal by ammonothermal treatment: reaction pathways, dynamics, and chemical stability. J. Am. Chem. Soc. 136, 11698–11706.

8. Hosono, H., Kim, J., Toda, Y., Kamiya, T., and Watanabe, S. (2017). Transparent amorphous oxide semiconductors for organic electronics: application to inverted oleds. Proc. Natl. Acad. Sci. U S A 114, 233–238.

9. Li, H., and Mahanti, S. (2004). Theoretical study of encapsulated alkali metal atoms in nanoporous channels of ITQ-4 zeolite: one-dimensional metals and inorganic electrides. Phys. Rev. Lett. 93, 216406.

10. Dye, J.L., Cram, K.D., Urbin, S.A., Redko, M.Y., Jackson, J.E., and Lefenfeld, M. (2005). Alkali metals plus silica gel: powerful reducing agents and convenient hydrogen sources. J. Am. Chem. Soc. 127, 9338–9339.

11. Lee, K., Kim, S.W., Toda, Y., Matsuishi, S., and Hosono, H. (2013). Dicalcium nitride as a two-dimensional electride with an anionic electron layer. Nature 494, 336–340.

12. Zhang, Y., Xiao, Z., Kamiya, T., and Hosono, H. (2015). Electron confinement in channel spaces for one-dimensional electride. J. Phys. Chem. Lett. 6, 4966–4971.

13. Zhang, Y., Wang, B., Xiao, Z., Lu, Y., Kamiya, T., Uwatoko, Y., Kageyama, H., and Hosono, H. (2017). Electride and superconductivity behaviors in Mn_5Si_3-type intermetallics. npj Quantum Mater. 2, 45.

14. Wang, J., Hanzawa, K., Hiramatsu, H., Kim, J., Umezawa, N., Iwanaka, K., Tada, T., and Hosono, H. (2017). Exploration of stable strontium phosphide-based electrides: theoretical structure prediction and experimental validation. J. Am. Chem. Soc. 139, 15668–15680.

15. Lu, Y., Tada, T., Toda, Y., Ueda, S., Yokoyama, T., Kitano, M., and Hosono, H. (2016). Water durable electride Y_5Si_3: electronic structure and catalytic activity for ammonia synthesis. J. Am. Chem. Soc. 138, 3970–3973.

16. Inoshita, T., Jeong, S., Hamada, N., and Hosono, H. (2014). Exploration for two-dimensional electrides via database screening and ab initio calculation. Phys. Rev. X 4, 031023.

17. Tada, T., Takemoto, S., Matsuishi, S., and Hosono, H. (2014). High-throughput ab initio screening for two-dimensional electride materials. Inorg. Chem. 53, 10347–10358.

18. Zhang, Y., Wang, H., Wang, Y., Zhang, L., and Ma, Y. (2017). Computer-assisted inverse design of inorganic electrides. Phys. Rev. X 7, 011017.

19. Burton, L.A., Ricci, F., Chen, W., Rignanese, G.-M., and Hautier, G. (2018). High-throughput identification of electrides from all known inorganic materials. Chem. Mater. 30, 7521–7526.

20. Pickard, C.J., and Needs, R.J. (2011). Predicted pressure-induced s-band ferromagnetism in alkali metals. Phys. Rev. Lett. 107, 087201.

21. Inoshita, T., Hamada, N., and Hosono, H. (2015). Ferromagnetic instability of interlayer floating electrons in the quasi-two-dimensional electride Y_2C. Phys. Rev. B 92, 201109.

22. Huang, H., Jin, K.-H., Zhang, S., and Liu, F. (2018). Topological electride Y_2C. Nano Lett. 18, 1972–1977.

23. Hirayama, M., Matsuishi, S., Hosono, H., and Murakami, S. (2018). Electrides as a new platform of topological materials. Phys. Rev. X 8, 031067.

24. Zhang, X., Guo, R., Jin, L., Dai, X., and Liu, G. (2018). Intermetallic Ca_3Pb: a topological zero-dimensional electride material. J. Mater. Chem. C 6, 575–581.

25. Park, C., Kim, S.W., and Yoon, M. (2018). First-principles prediction of new electrides with nontrivial band topology based on one-dimensional building blocks. Phys. Rev. Lett. 120, 026401.

26. Zhu, S.-C., Wang, L., Qu, J.-Y., Wang, J.-J., Frolov, T., Chen, X.-Q., and Zhu, Q. (2019). Computational design of flexible electrides with nontrivial band topology. Phys. Rev. Mater. 3, 024205.

27. Pickard, C.J., and Needs, R. (2009). Dense low-coordination phases of lithium. Phys. Rev. Lett. 102, 146401.

28. Matsuoka, T., and Shimizu, K. (2009). Direct observation of a pressure-induced metal-to-semiconductor transition in lithium. Nature 458, 186.

29. Ma, Y., Eremets, M., Oganov, A.R., Xie, Y., Trojan, I., Medvedev, S., Lyakhov, A.O., Valle, M., and Prakapenka, V. (2009). Transparent dense sodium. Nature 458, 182.

30. Dong, X., Oganov, A.R., Goncharov, A.F., Stavrou, E., Lobanov, S., Saleh, G., Qian, G.R., Zhu, Q., Gatti, C., Deringer, V.L., et al. (2017). A stable compound of helium and sodium at high pressure. Nat. Chem. 9, 440–445.

31. Zhu, Q., Oganov, A.R., and Lyakhov, A.O. (2013). Novel stable compounds in the Mg-O system under high pressure. Phys. Chem. Chem. Phys. 15, 7696–7700.

32. Lv, J., Wang, Y., Zhu, L., and Ma, Y. (2011). Predicted novel high-pressure phases of lithium. Phys. Rev. Lett. 106, 015503.

33. Shimizu, K., Ishikawa, H., Takao, D., Yagi, T., and Amaya, K. (2002). Superconductivity in compressed lithium at 20 k. Nature 419, 597.

34. F.H. Allen, G. Bergerhoff, and R. Sievers, eds. (1987). Crystallographic Databases (International Union of Crystallography), pp. 77–95.

35. Curtarolo, S., Hart, G.L., Nardelli, M.B., Mingo, N., Sanvito, S., and Levy, O. (2013). The high-throughput highway to computational materials design. Nat. Mater. 12, 191.

36. Jain, A., Ong, S.P., Hautier, G., Chen, W., Richards, W.D., Dacek, S., Cholia, S., Gunter, D., Skinner, D., Ceder, G., and Persson, K.A. (2013). Commentary: the materials project: a materials genome approach to accelerating materials innovation. Apl Mater. 1, 011002.

37. Zhao, S., Kan, E., and Li, Z. (2016). Electride: from computational characterization to theoretical design. Wiley Interdiscip. Rev. Comput. Mol. Sci. 6, 430–440.

38. Dale, S.G., and Johnson, E.R. (2018). Theoretical descriptors of electrides. J. Phys. Chem. A 122, 9371–9391.

39. Becke, A.D., and Edgecombe, K.E. (1990). A simple measure of electron localization in

Matter

CellPress

atomic and molecular systems. J. Chem. Phys. 92, 5397–5403.

40. Bader, R.F.W. (1990). Atoms in Molecules—A Quantum Theory (Oxford University Press).

41. Henkelman, G., Arnaldsson, A., and Jonsson, H. (2006). A fast and robust algorithm for bader decomposition of charge density. Comput. Mater. Sci. 36, 354–360.

42. Mizoguchi, H., Park, S.W., Kishida, K., Kitano, M., Kim, J., Sasase, M., Honda, T., Ikeda, K., Otomo, T., and Hosono, H. (2019). Zeolitic intermetallics: Lnnisi (ln = la - nd). J. Am. Chem. Soc. 141, 3376–3379.

43. Wu, J., Li, J., Gong, Y., Kitano, M., Inoshita, T., and Hosono, H. (2019). Intermetallic electride catalyst as a platform for ammonia synthesis. Angew. Chem. Int. Ed. 58, 825–829.

44. Walsh, A., and Scanlon, D.O. (2013). Electron excess in alkaline earth sub-nitrides: 2d electron gas or 3d electride? J. Mater. Chem. C 1, 3525–3528.

45. Oganov, A.R., Pickard, C.J., Zhu, Q., and Needs, R.J. (2019). Structure prediction drives materials discovery. Nat. Rev. Mater. https://doi.org/10.1038/s41578-019-0101-8.

46. Miao, M.-S., and Hoffmann, R. (2014). High pressure electrides: a predictive chemical and physical theory. Acc. Chem. Res. 47, 1311–1317.

47. Schneider, S.B., Seibald, M., Deringer, V.L., Stoffel, R.P., Frankovsky, R., Friederichs, G.M., Laqua, H., Duppel, V., Jeschke, G., Dronskowski, R., and Schnick, W. (2013). High-pressure synthesis and characterization of $Li_2Ca_3[N_2]_3$: an uncommon metallic diazenide with $[N_2]^{2-}$ ions. J. Am. Chem. Soc. 135, 16668–16679.

48. Madsen, G.K., Iversen, B.B., Blaha, P., and Schwarz, K. (2001). Electronic structure of the sodium and potassium electrosodalites (Na/K)$_8$(AlSiO$_4$)$_6$. Phys. Rev. B 64, 195102.

49. Zhang, T., Jiang, Y., Song, Z., Huang, H., He, Y., Fang, Z., Weng, H., and Fang, C. (2019). Catalogue of topological electronic materials. Nature 566, 475–479.

50. Vergniory, M.G., Elcoro, L., Felser, C., Regnault, N., Bernevig, B.A., and Wang, Z. (2019). A complete catalogue of high-quality topological materials. Nature 566, 480–485.

51. Tang, F., Po, H.C., Vishwanath, A., and Wan, X. (2019). Comprehensive search for topological materials using symmetry indicators. Nature 566, 486–489.

52. Liu, J., and Vanderbilt, D. (2014). Spin-orbit spillage as a measure of band inversion in insulators. Phys. Rev. B 90, 125133.

53. Choudhary, K., Garrity, K.F., and Tavazza, F. (2018). High-throughput discovery of topological materials using spin-orbit spillage. Sci. Rep. 9, https://doi.org/10.1038/s41598-019-45028-y.

54. Wang, J., Zhu, Q., Wang, Z., and Hosono, H. (2019). Ternary inorganic electrides with mixed bonding. Phys. Rev. B 99, 064104.

55. Qu, J., Zhu, S., Zhang, W., and Zhu, Q. (2019). Electrides with dinitrogen ligands. ACS Appl. Mater. Interfaces 11, 5256–5263.

56. Vajenine, G.V., and Simon, A. (2001). NaBa$_2$O: a fresh perspective in suboxide chemistry. Angew. Chem. Int. Ed. 40, 4220–4222.

57. Wan, B., Lu, Y., Xiao, Z., Muraba, Y., Kim, J., Huang, D., Wu, L., Gou, H., Zhang, J., Gao, F., et al. (2018). Identifying quasi-2D and 1D electrides in yttrium and scandium chlorides via geometrical identification. npj Comput. Mater. 4, 77.

58. Muhammad, S., Xu, H., Liao, Y., Kan, Y., and Su, Z. (2009). Quantum mechanical design and structure of the li@b10h14 basket with a remarkably enhanced electro-optical response. J. Am. Chem. Soc. 131, 11833–11840.

59. Zhong, R.-L., Xu, H.-L., Li, Z.-R., and Su, Z.-M. (2015). Role of excess electrons in nonlinear optical response. J. Phys. Chem. Lett. 6, 612–619.

60. Kim, S.W., Toda, Y., Hayashi, K., Hirano, M., and Hosono, H. (2006). Synthesis of a room temperature stable 12CaO·7Al$_2$O$_3$ electride from the melt and its application as an electron field emitter. Chem. Mater. 18, 1938–1944.

61. Kresse, G., and Furthmüller, J. (1996). Efficient iterative schemes for ab initio total-energy calculations using a plane-wave basis set. Phys. Rev. B 54, 11169–11186.

62. Perdew, J.P., Burke, K., and Ernzerhof, M. (1996). Generalized gradient approximation made simple. Phys. Rev. Lett. 77, 3865–3868.

63. Ong, S.P., Richards, W.D., Jain, A., Hautier, G., Kocher, M., Cholia, S., Gunter, D., Chevrier, V.L., Persson, K.A., and Ceder, G. (2013). Python Materials Genomics (pymatgen): a robust, open-source python library for materials analysis. Comput. Mater. Sci. 68, 314–319.